PORT SAID ENGINEERING RESEARCH JOURNAL

Faculty of Engineering - Port Said University

Volume 29 No. 1 pp: 51:68

Simplified Modeling of Unstiffened End-plate Connections in Nonlinear Analysis of Steel Frames at Elevated Temperatures

Ashraf ElSabbagh [1], Waleed Nassef [2], Mohamed Elghandour [3], Tarek Sharaf [4]*

[1] *Associate Prof., Civil Engineering Department, Faculty of Engineering, Port Said University, Port Said, Egypt, email: ashref.ismail@eng.psu.edu.eg*

[2] *Ph.D. Candidate, Civil Engineering Department, Faculty of Engineering, Port Said University, Port Said, Egypt, email: w.m.nassef@gmail.com*

[3] *Professor, Civil Engineering Department, Faculty of Engineering, Port Said University, Port Said, Egypt, email: dr.elghandor@gmail.com*

[4] *Associate Prof., Civil Engineering Department, Faculty of Engineering, Port Said University, Port Said, Egypt, email: tarek.sharaf@eng.psu.edu.eg*

[*] *Corresponding author,* *DOI: 10.21608/PSERJ.2024.315330.1362*

Received 26-8-2024

Revised 21-10-2024

Accepted 5-11-2024

ABSTRACT

This work presents a simplified procedure for modeling the moment-rotation relationship of extended end-plate (EEP) and flush end-plate (FEP) connections at both ambient and elevated temperatures, to be incorporated in global frame analysis. The main interest of this paper is to offer a swift numerical routine providing direct application, reasonable accuracy, and analysis time saving. The procedure is divided into three main stages: estimating the initial joint characteristics at ambient temperature, updating those characteristics at elevated temperatures, and choosing a suitable mathematical representation of the moment-rotation curve. Regression analysis of experimental test database was applied to generate empirical formulae for estimation of the initial stiffness and moment strength of end-plate connections. Additionally, a parametric analysis routine, based on the Eurocode component method (CM) for a practical range of end-plate connection configurations, is utilized to enrich the database and to estimate the behavior of connections that are not existing in the database. The proposed formulae involve the geometrical and material parameters that have major influence on connection characteristics. The explicit presence of the material parameters in the proposed formulae enables the procedure to be extended to consider the effect of elevated temperatures. Two power models were discussed, suggested and compared to generate full moment-rotation curve of connections at both ambient and elevated temperatures. Moreover, the proposed procedure was applied and validated against previous work and showed good accuracy and low analysis time.

Keywords: Steel Connections, Nonlinear Analysis, Steel Frames, Moment-Rotation Relationship, Elevated Temperatures.

1. INTRODUCTION

Advanced analysis of steel frames necessitates considering realistic characteristics of connections rather than the idealized pinned or rigid models. Moreover, most design codes require considering the rotational behavior of connections in the global frame analysis, especially in inelastic and large deformation analyses [1, 2]. On the other hand, temperature rise caused by fire has significant effects on joint characteristics, which increase the complexity of the analysis. At elevated temperatures, thermal expansion and material degradation mostly impose the utilization of both types of nonlinear analysis. Despite the most reliable way to determine connection characteristics is experimental testing, fire tests are extremely expensive and rather troublesome due to furnace limitations. The numerical alternative represented by finite element modeling is fairly efficient yet time consuming, especially in fire simulation problems; its computational cost limits their utilization in everyday practice.

Hence, an efficient and simple model for representing the nonlinear behavior of connection is highly required. Still, the connection characteristics at elevated temperatures need to be predicted and implemented in the analysis. Those characteristics are namely, initial stiffness, moment capacity and rotation capacity. The focus in this study is on the first two characteristics, as the ductility of a connection can be guaranteed by controlling some of the connection's components, i.e., end-plate thickness and/or column flange thickness, to assure that the rotation capacity is higher than the required for a specific connection [3, 4, 5].

Over the last century, numerous research studies proposed predictive models of connection behavior at ambient temperature. Various approaches have been used to obtain the moment–rotation curve of steel connections including experimental, mechanical, analytical, empirical, and numerical [1, 2]. Experimental tests provide the most accurate knowledge of connection behavior; yet they are too expensive for everyday practice and are mostly reserved for scientific research purposes only [2].

In the USA, the Steel Connection Data Bank (SCDB) was developed via collecting the experimental tests results from over 349 tests have been carried out since 1936 till 1995 from all over the world [6, 7]. Moreover, (SCDB) program was developed for providing mathematical representation of all experimental moment–rotation curves [8]. Similarly, SERICON data bank was developed by Arbed Recherches and Aachen University in 1992 [9]. This data bank included only European test results and contained tests on single joint components as well as composite connections. The work continued and the data bank was expanded to produce the SERICON II database in 1998 by Cruz *et al.* [10].

Empirical formulations relate the parameters which represent mathematically the moment–rotation curve to the geometrical and material configurations of connections [2]. These formulations can be usually obtained by means of regression analysis of experimental testing, finite element (FE) parametric analyses, or mechanical models. One of the earliest models is the odd-power polynomial representation of the moment–rotation curve which was introduced by Frye and Morris [11]. The main downside in this formulation is that the formulation is based on general geometrical dimensions of the connection and neglects important details of the connection [1] and the model error is extremely high [12]. Krishnamurthy *et al.* [13, 14] introduced an empirical model based on a wide FE parametric study on the rotational behavior of end-plate connections. The downside is that the engaged parameters are independent of the column's geometry since it was considered in the FE model. Based on regression analysis of fully documented experimental test results and extensive numerical simulations, Kozlowski *et al.* [15] presented a simple empirical model for the prediction of the initial stiffness as well as moment capacity of various types of bare steel and composite joints, utilizing data generated by the Eurocode 3 component method (CM). The analysis indicates that the initial stiffness and moment capacity of steel joint depends mainly on four parameters: the height of beam and column sections, bolt diameter and end-plate thickness. The downside of the proposed formulae that they are limited to IPE beams and HEB column sections only. Terracciano *et al.* [16] also proposed a similar empirical model based on the regression analysis of parametric predictions generated by the Eurocode 3 component method. The drawback of this model was it is limited to steel grade S275 and grade 8.8 bolts and restricted by geometrical constraints ($t_p = t_{fc}$). Based on a 3D FE parametric study of 180 specimens, Eladly and Schafer [17] proposed a predictive empirical model for generating full moment-rotation curve of exterior stainless-steel EEPs. The model is limited to connections with relatively thin end plates ($t_p = 8 - 12$ mm), small bolts ($d = 12 - 16$ mm), and shallow beams ($h_b = 240 - 300$ mm). Material properties are explicitly considered in this model as an advantage over the other models. Kong *et al.* [18] derived new semi-empirical equations for predicting the initial stiffness and ultimate moment of flush end-plate connections using finite element (FE) analyses. The study suggested a new type of fracture mechanism for flush end-plate connections which was verified through comparison with previous experimental studies, showing good agreement with experimental data.

More recently, and by utilizing the approaches of artificial neural network (ANN) and multi-linear regression, Kueh [19] presented explicit expressions for moment capacity and initial stiffness of steel flush end-plate (FEP) beam-column connections in terms of beam dimensions (depth, width, flange thickness, and web thickness), column dimensions (depth, and width), end-plate dimensions (depth, and thickness), and bolt capacity. The proposed formulae gave good predictions and can be extended to other type of connections. Likewise, Georgiou and Elkady [20] developed an ANN procedure capable of predicting the initial rotational stiffness, moment capacity, and post-yield stiffness of (FEP) connections employing of thirteen geometric, material, and layout features. This procedure provides higher prediction accuracy compared with the pure empirical approaches. Further information and comparisons of empirical predictive models can be found in [2, 21, 22].

Regarding the connection behavior at elevated temperatures, El-Rimawi *et al.* [23] outlined the basis for studying the influence of connection stiffness on the behavior of steel beams in fire, utilizing Ramberg-Osgood formulation in representation the connection response at high temperatures. Al-Jabri *et al.* [24] conducted a series of elevated temperature tests on beam-to-column connections and presented moment-

rotation-temperature curves for a variety of connections, using a modified Ramberg–Osgood expression. Da silva *et al.* [25] extended the component method to predict analytically the response of steel joints under fire loading, using bi-linear approximation of the mechanical models consisting of extensional springs and rigid links. The analytical procedure could predict the moment–rotation response under fire conditions. An application to a cruciform flush end-plate beam-to-column steel joint was presented and compared to the experimental results, previously tested by Al-Jabri *et al*. [24] under various loading conditions. Valuable results have been drawn from other studies are referred to in the subsequent sections. Nevertheless, additional experimental testing and extensive numerical simulations are recommended to building reliable database of moment-rotation-temperature data of steel connections at high temperatures.

In the case of conventional analysis, the design procedure for a connection is necessarily iterative despite it is executed afterwards: a configuration of joint components is selected; the resistance of that configuration is evaluated; the configuration is then modified for greater resistance or greater economy, until a satisfactory solution is achieved [26]. The situation is further complex in nonlinear analysis at high temperatures; more iteration is essentially required during the formulation of the elemental tangential stiffness.

Most of the previous predictive models have some sort of limitation including material, geometrical, and positional limitations. Additionally, and to the authors' knowledge, just few studies have proposed a complete procedure for estimating connection behavior at elevated temperatures. Besides, most of these studies were limited to specific connection configurations. Accordingly, the main objective of this study is to develop a simple and direct procedure that represents the moment-rotation relationship of moment-resistant connections at high temperatures. This procedure aims to overcome the limitations of previous predictive models, with sufficient efficiency and accuracy, to be incorporated into the everyday analyses.

Notation List

b_p width of the end-plate;

d nominal diameter of the bolts;

E Young's modulus;

f_{ub} ultimate tensile strength of the bolts;

f_y yield stress of connection components;

h_b height of the beam section;

h_c height of the column section;

$k_{b,\theta}$ Eurocode reduction factor for bolt strength with temperature

$k_{E,\theta}$ Eurocode reduction factor for Young's modulus with temperature

$k_{y,\theta}$ Eurocode reduction factor for carbon steel strength with temperature

M_L reference (limiting) moment;

$M_{j,Rd}$ design moment resistance of the connection;

n curve sharpness/shape parameter;

p vertical distance of bolts (pitch);

p_{1-2} vertical distance between first and second bolt rows;

p_{2-3} vertical distance between second and third bolt rows;

$R_E(T)$ Reduction factor function for Young's modulus with temperature

$R_f(T)$ Reduction factor function for carbon steel strength with temperature

R_m^2 coefficient of determination for moment capacity;

R_s^2 coefficient of determination for initial stiffness;

s_f weld thickness;

$S_{j,ini}$ the initial rotational stiffness of the connection;

$S_{j,p-l}$ the post-yield rotational stiffness of the connection;

t_{fc} thickness of the column flange;

t_p thickness of the end-plate;

T temperature in centigrade;

w horizontal distance of bolts (gauge);

β transformation parameter;

ϕ rotation of the connection;

2. CONNECTION CHARACTERISTICS AT AMBIENT TEMPERATURE

Since unstiffened extended and flush end-plate beam-to-column connections exhibit semi-rigid behavior, the present study focuses on such types of connections. Figure 1 shows typical configuration of extended and flush end-plate joints.

In the past decades, hundreds of experimental test programs have been conducted to assess the behavior of different types of steel connections; the results of those tests were collected and tabulated in the form of database [8, 12]. After excluding the test results out of interest from the database, the number of the selected test results in concern is found to be limited; besides, the majority of

tests engaged connections built-up from mild carbon steel. Consequently, the available database needed to be enriched using a different source. This source can be either a numerical parametric study using FE analysis or an analytical mechanical model.

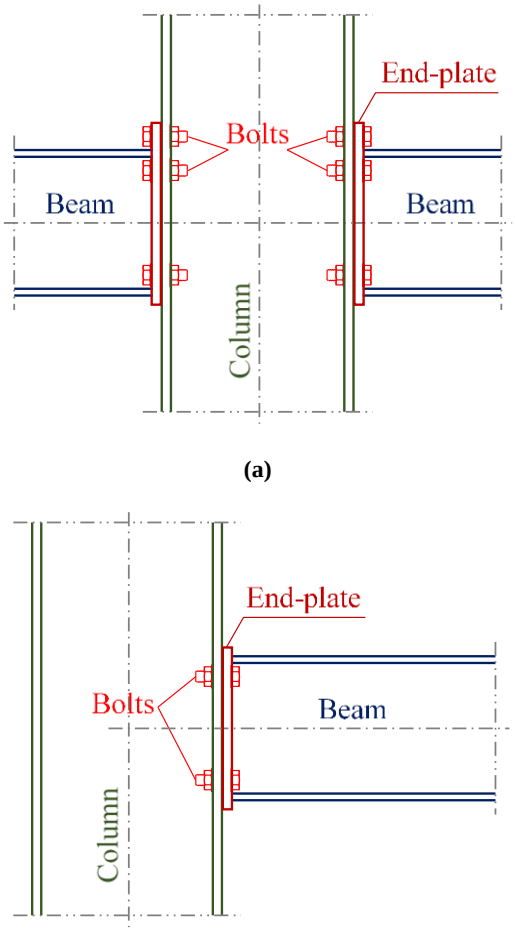

Figure 1: Typical end-plate joints; a) internal extended end-plate joint with two bolt rows in tension, b) external flush end-plate joint with one bolt row in tension.

In the mechanical models, the joint is represented by using a combination of selected flexible and rigid components, which in turn are modeled mathematically using their stiffness and resistance values. These values are usually obtained from empirical relationships by either elastic or inelastic constitutive laws for the spring elements [25]. The most suitable and widely used model is the Eurocode component method (CM) [27], in which it is possible to predict, with sufficient accuracy, the rotational stiffness and moment capacity of semi-rigid joints, especially when the joint is subjected primarily to bending moment with minimal axial force [2, 28]. Statistical assessment of the CM indicates that it provides satisfactory and reliable predictions of joint moment capacity, despite the initial rotational stiffness tends to be overestimated. However, the CM is commonly categorized by practitioners as being time-consuming for practical applications, especially when iterative procedures are expected [16].

2.1. The Component Method

The component method consists of modeling the connection as a set of basic components (i.e., extensional springs and rigid links). Each component/spring represents a specific part of the connection and has its own resistance and stiffness to tension, compression, and shear, depending on the type of loading. In addition to nut stripping, failure of each of those components will lead to entire connection failure [29]. Hence, the mechanical behavior of each component is evaluated and characterized individually. The Eurocode 3 part 1-8 [27] offers 20 basic components to be considered in the evaluation of steel connections, depending on the connection type and configuration. Figure 2-a and Table 1 summarize the active components of end-plate connections.

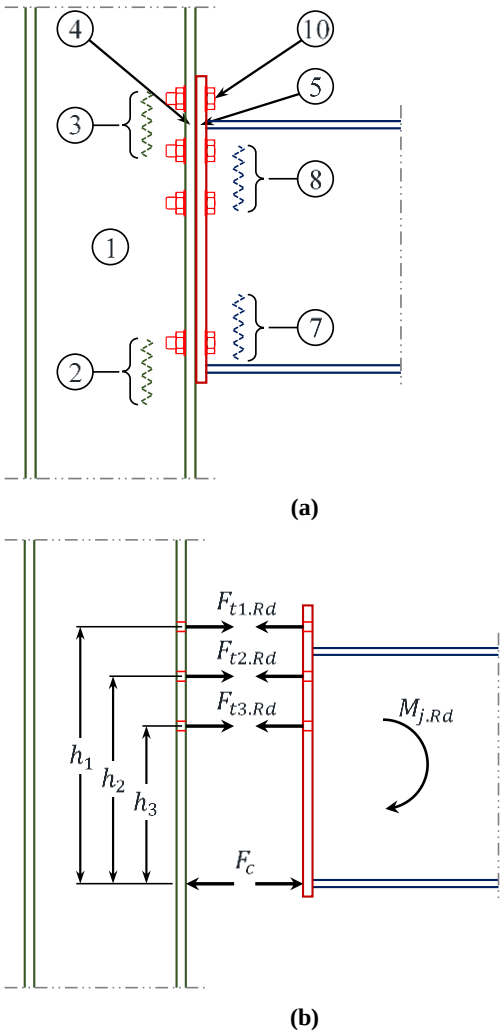

Figure 2: (a) Moment resisting components of extended end-plate connection, and (b) distribution of forces on the connection [27].

For simplicity, the weld between the end-plate and both flanges are assumed to be continuous full strength groove weld while the weld between section web and end-plate is considered as fillet weld with sufficient throat thickness. Accordingly, the behavior of weld is omitted in the present study. In addition, the bolt preload parameter is not considered as it is commonly ignored in such empirical predictive models to maintain simplicity [20].

The total resistance and stiffness of the connection are then obtained from the resistances of the assembly of its components. The moment resistance $M_{j.Rd}$ of end-plate type of connections can be determined using Equation (1) as [27]:

$$M_{j.Rd} = \sum_r h_r . F_{rt.Rd} \quad (1)$$

where r identifies the tension bolt row number, $F_{rt.Rd}$ is the (weakest) tension resistance of bolt row r, and h_r is the lever arm of bolt row r measured from the adopted center of compression, as shown in Figure 2-b. For calculating the initial rotational stiffness $S_{j.ini}$ of the connection, it is at first required to calculate the effective stiffness of the springs in series for each bolt row. Subsequently, the total equivalent stiffness of all bolt rows in parallel can be calculated. Finally, the initial rotational stiffness can be expressed in Equation (2) as [27]:

$$S_{j.ini} = \frac{E z^2}{\frac{1}{k_1} + \frac{1}{k_2} + \frac{1}{k_{eq}}} \quad (2)$$

where E is Young's modulus of steel, k_1 and k_2 are the stiffness values of components 1 and 2, z is the lever arm calculated from the center of compression, and k_{eq} is the equivalent stiffness of the tension components.

Table 1. List of the active components of end-plate moment connections.

Ref.	Component
1	Column web panel in shear
2	Column web in compression
3	Column web in tension
4	Column flange in bending
5	Endplate in bending
7	Beam web in compression
8	Beam web in tension
10	Bolts in tension

With proper mathematical model, full moment-rotation curve can be generated using both initial stiffness and moment capacity of the joint, as will be discussed in the following section. That overcomes the need of implementing complex nonlinear finite element analysis to predict the moment–rotation response of steel joints. It is still necessary to supply the analysis engineers with a simple complete procedure of modeling semi-rigid joints in their analyses [30].

2.2. Identifying of the High-impact Parameters

Majority of the studies that investigated the influence of geometrical connections configuration on their initial stiffness and moment resistance agreed that the following parameters have a remarkable impact on connection characteristics:

- End-plate thickness t_p,
- End-plate width b_p,
- Beam section height h_b,
- Column section height h_c,
- Column flange thickness t_{fc},
- Horizontal spacing of bolts (gauge) w,
- Vertical spacing of bolts (pitch) p,
- Diameter and grade of bolts d and f_{ub}.

Essentially, the most significant parameters are; beam height h_b, end-plate thickness t_p, bolt diameter d. In addition, the selected column section parameter, taken as column section height h_c in some approaches and column flange thickness t_{fc} in others and are considered in the present work [15, 19]. Figure 3 depicts the geometric parameter definition of end-plate connections.

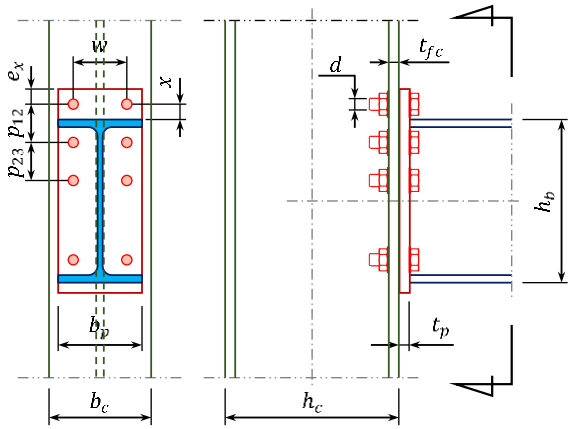

Figure 3: Identifying of the geometric parameters of end-plate connection.

2.3. Definition of Joint Parameters

Developing an empirical model requires building a connection database that covers a wide range of the practical geometric parameters to be involved. For that purpose, an automated parametric routine that follows the Eurocode analysis procedures was built and used to generate the required database. The analysis matrix was set to:

- Column: HEB sections ranges from HEB140 to HEB400,
- Beam: IPE sections ranges from IPE200 to IPE600 (provided that: $1 \leq h_b/h_c \leq 1.5$) ,
- End-plate: $t_p \in (10,12,15,20,25)$ mm (provided that: $t_{fb} \leq t_p \leq t_{fc}$),
- Bolts: $d \in (12,16,20,24,27)$ mm (provided that: $0.8t_p \leq d \leq 1.5t_p$),
- Bolt grades: 8.8 and 10.9,
- Steel grades: S235, S275, and S355 ($E = 210\ GPa$) for all connection components.

While the values of the other geometrical properties (e.g. $b_p, w, p, e_x, x, \dots$), see Figure 3, were kept in the practical range and were proportional to the major as follows: $b_p = (b_c + b_b)/2$, $p_{1-2} = \max(3d + t_{fb}, 2x + t_{fb})$, $p_{2-3} = 3d$, $w = b_p/2$, $x = 1.5d + s_f$, and $e_x = 1.5d$.

Moreover, the routine was designated to calculate the moment capacity and the initial stiffness for the external and internal joints (via the parameter β), and different setups of tension bolt rows, see Figure 1. The designations of the eight connection types under investigation are listed in Table (2).

2.4. The Proposed Formulae

In addition to the test results in the available database, considerably large data were extracted by running the routine on the eight connection types with various geometric parameters that were defined in the previous sub-section. Regression analyses using IBM® SPSS [31] were utilized to produce the following formulae:

$$M_{j.Rd}(20) = a.f_y^b.h_b^c.t_{fc}^e.f_{ub}^f.d^g.t_p^h \quad (3)$$

$$S_{j.ini}(20) = k.h_b^l.t_{fc}^m.d^u.t_p^o + q \quad (4)$$

where $M_{j.Rd}(20)$ and $S_{j.ini}(20)$ are, respectively, the moment capacity and initial stiffness at ambient temperature and $(a, b, c, e, f, g, h, k, l, m, u, o, and\ q)$ are the equations' constants obtained by the regression analysis to describe Equations (3) and (4). These constants are listed in Tables 3 and 4.

Figures 4 and 5 show data regression analysis of the direct estimated connection characteristics using the proposed formulae against the stepwise application of the component method (CM) for various connection configuration and steel grades. The graphs show very good agreement and indicate that the proposed formulae can provide a direct alternate of the component method stepwise procedure.

Table 2. Designations of moment-resistant connections in the present study.

Connection Location	Connection Type	Number of Bolt Rows in Tension	Designation
External	Extended EP	3	EE3
External	Extended EP	2	EE2
External	Flush EP	2	EF2
External	Flush EP	1	EF1
Internal	Extended EP	3	IE3
Internal	Extended EP	2	IE2
Internal	Flush EP	2	IF2
Internal	Flush EP	1	IF1

Table 3. External joints' constants of Equations (3) and (4).

Constant	Joint Designation			
	EE3	EE2	EF2	EF1
a	6.73×10^{-6}	2.63×10^{-6}	7.38×10^{-7}	5.44×10^{-7}
b	0.460	0.328	0.332	0.229
c	1.123	1.040	1.230	1.123
e	0.626	0.284	0.225	0.062
f	0.388	0.621	0.623	0.766
g	0.773	1.216	1.174	1.495
h	0.413	0.464	0.514	0.386
k	0.3086	0.4166	0.0135	0.0177
l	1.585	1.544	2.075	1.965
m	0.649	0.569	0.428	0.273
u	0.149	0.207	0.075	0.255
o	0.125	0.156	0.268	0.360
q	-4065	-4283	-690	-38

Table 4. Internal joints' constants of Equations (3) and (4).

Constant	Joint Designation			
	IE3	**IE2**	**IF2**	**IF1**
a	3.42×10^{-6}	2.19×10^{-6}	6.20×10^{-7}	5.20×10^{-7}
b	0.400	0.278	0.277	0.232
c	1.131	1.032	1.231	1.116
e	0.291	0.101	0.043	0.048
f	0.524	0.716	0.717	0.775
g	1.043	1.300	1.261	1.505
h	0.527	0.525	0.562	0.392
k	0.1503	0.2390	0.0062	0.0093
l	2.108	2.019	2.497	2.292
m	-0.243	-0.266	-0.329	-0.334
u	0.288	0.329	0.254	0.414
o	0.252	0.272	0.397	0.471
q	-1730	-2829	833	1131

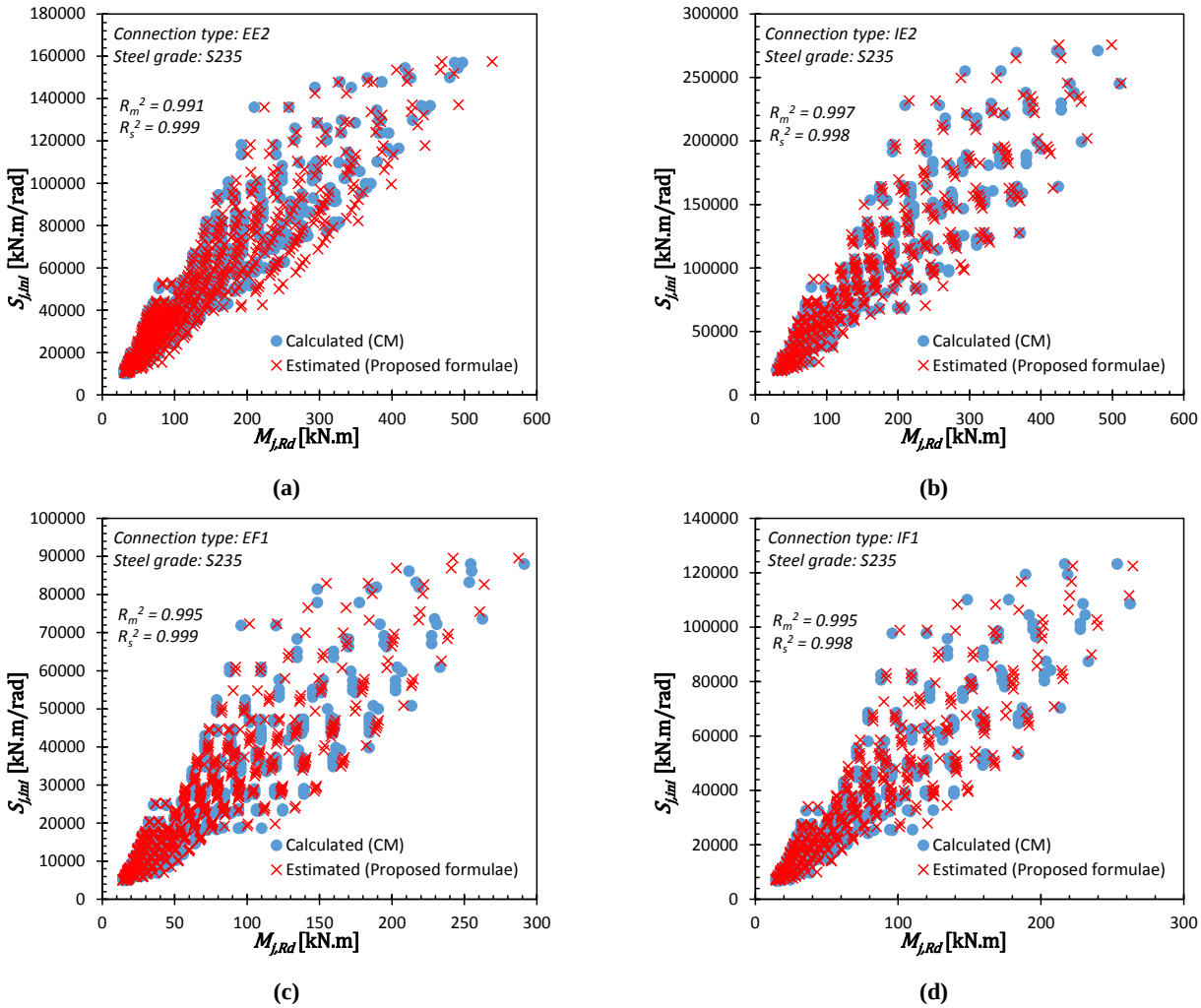

Figure 4: Data regression analysis of $M_{j.Rd}$ and $S_{j.ini}$ for S235 connections; (a) EE2, (b) IE2, (c) EF1, and (d) IF1.

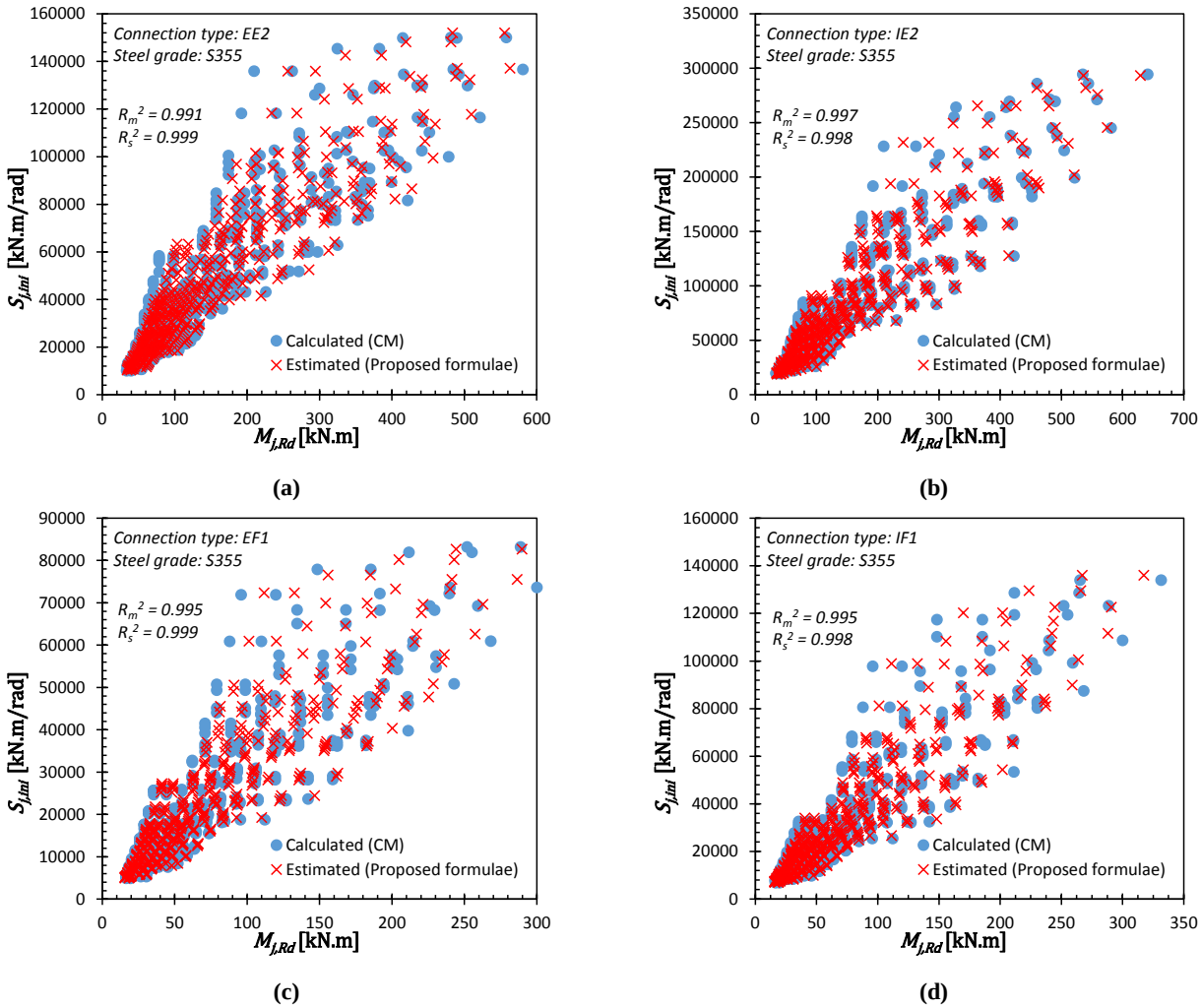

Figure 5: Data regression analysis of $M_{j.Rd}$ and $S_{j.ini}$ for S355 connections; (a) EE2, (b) IE2, (c) EF1, and (d) IF1.

2.5. Validation of the Proposed Formulae

In order to verify the proposed formulae at ambient temperature, a set of comparisons with selected fully documented test results are presented. Table 5 lists the parameters of each experiment and Figures 6 to 13 compare graphically the moment-rotation curve of each test (solid line), the estimated initial stiffness (dashed line), and the estimated moment capacity (dash-dot line).

Table 5. Parameters of experimental tests on end-plate connections.

Test ID	Joint Designation	Beam Section	Column Section	f_y* [MPa]	t_p [mm]	Bolt Size	Bolt Grade
Ostrander, Test 1	EF2	W10 × 21	W8 × 28	313	12.5	3/4 “	A325
Ostrander, Test 11	EF2	W10 × 21	W8 × 40	433	9.5	3/4 “	A325
Zoetemeijer and Kolstein, Test 14	EF2	IPE300	HEA240	300	25	M24	8.8
de Lima 2004	EE2	IPE240	HEB240	370	15	M20	10.9
Zoetemeijer, Test M3A	EE3	IPE300	HEA240	264	22	M20	10.9
Graham, Test CS1-1	EE3	UB 356×171×45	UC 203×203×86	230	15	M16	8.8
Zoetemeijer and Munter, Test 1	EE3	IPE400	HEA240	232	20.5	M20	8.8
Tong, Test 4	EE3	UB 305×165×54	UC 254×254×132	300	12	M20	8.8

* Measured yield stress of the end-plate.

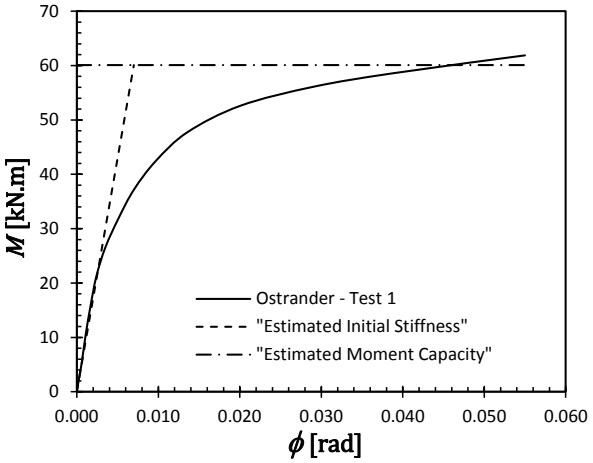

Figure 6: Comparison of the proposed formulae with FEP test "Ostrander – Test 1" [32].

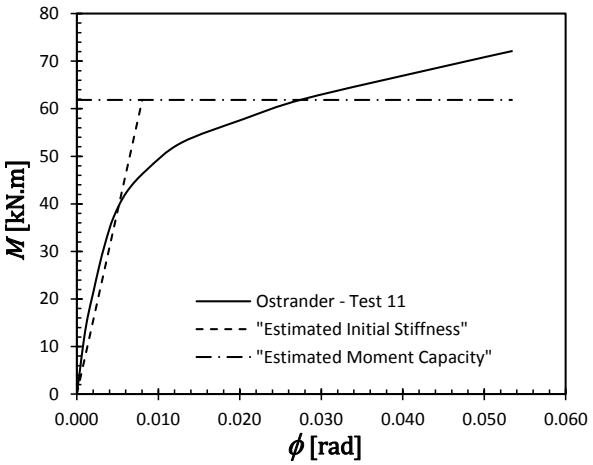

Figure 7: Comparison of the proposed formulae with FEP test "Ostrander – Test 11" [32].

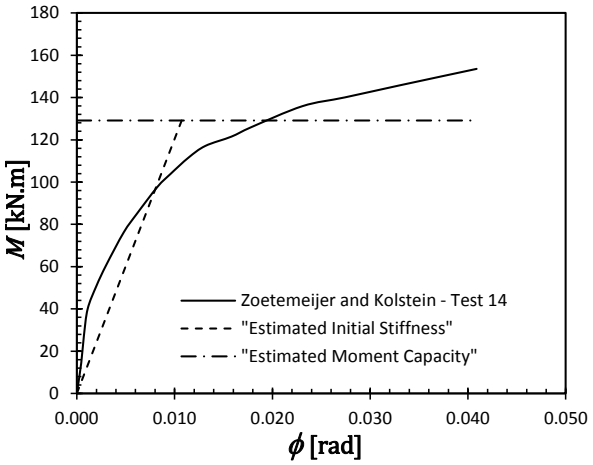

Figure 8: Comparison of the proposed formulae with FEP test "Zoetemeijer and Kolstein - Test 14" [32].

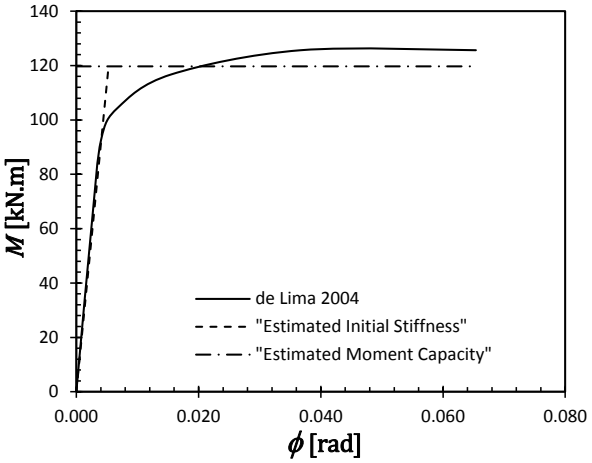

Figure 9: Comparison of the proposed formulae with EEP test "de Lima 2004" [28].

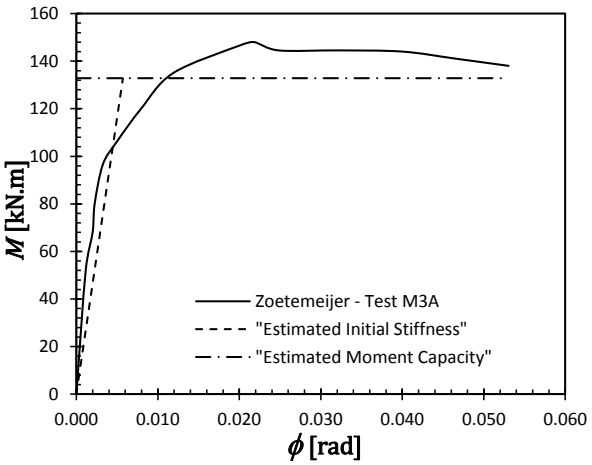

Figure 10: Comparison of the proposed formulae with EEP test "Zoetemeijer - Test M3A" [32].

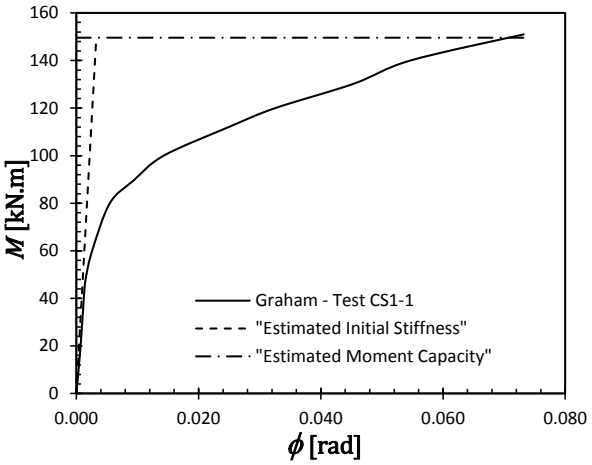

Figure 11: Comparison of the proposed formulae with EEP test "Graham – Test CS1-1" [32].

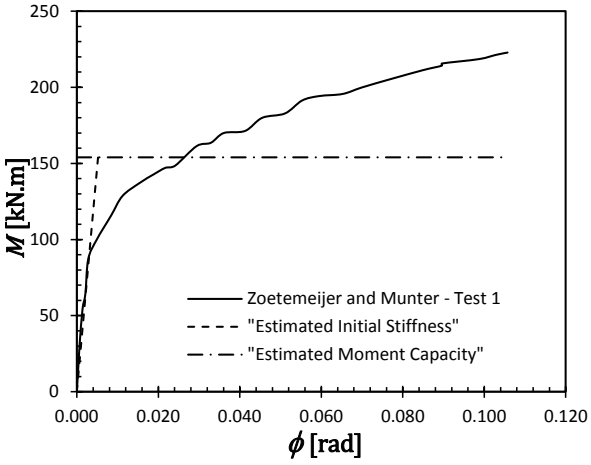

Figure 12: Comparison of the proposed formulae with EEP test "Zoetemeijer and Munter - Test 1" [32].

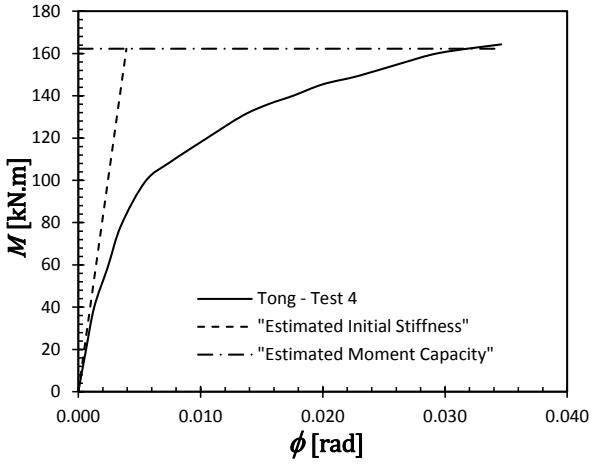

Figure 13: Comparison of the proposed formulae with EEP test "Tong – Test 4" [32].

Moreover, as may be noticed from Table 5, the proposed formulae are valid and applicable on most I- and H-shaped sections and different values of yield stress.

As can be deduced from Figures 6 to 13, the proposed formulae provide reasonable estimations compared to experimental tests. Though, some estimations are not consistently accurate as expected considering the simplifications associated with empirical models [22]. This drawback may be mitigated by proper calibration, as discussed in Section 3. However, the proposed prediction model almost coincides with the results obtained by the stepwise application of CM which is a worldwide accepted design approach, see Figures 4 and 5. The coefficient of determination R^2, that measures goodness of fit of a model, exceeds 0.99 for the equations of $M_{j.Rd}$ and $S_{j.ini}$ for all connection types. The precise values of R_m^2 (for moment capacity) and R_s^2 (for initial stiffness) are included in each plot of Figures 4 and 5.

2.6. Advantages of the proposed formulae

The proposed predictive formulae are intended to overcome the drawbacks of the existing predictive models, as most models were developed based on a specific material grade or limited geometric configurations. Table 6 provides a comparison of the proposed formulae with other models.

Table 6. Comparison between the main features of the proposed model and other predictive models.

Predictive Model Name	Kozlowski *et al.* [15]	Terracciano *et al.* [16]	Eladly and Schafer [17]	The proposed model
Connection Types	FEP and EEP	EEP	Stainless EEP	FEP and EEP
Connection Position	External and Internal	Splice	External	External and Internal
Data Source	Parametric CM	Parametric CM	Parametric 3D FE	Parametric CM
Dimensional Constraints	Average	High	High	Low
Material Parameter	Steel S235	Steel S275	Explicitly included	Explicitly included
Applicability to Elevated Temperatures	No	No	No	Yes

3. MATHEMATICAL REPRESENTATION OF MOMENT-ROTATION CURVE

In the bi-linear model, initial stiffness and moment capacity are sufficient to represent full moment-rotation curve. However, to consider the gradual yielding of the connection, other parameters are required to fully describe the curve; these are; rotation capacity, post-yield rotational stiffness, and curve sharpness, as the depicted in Figure 14. Therefore, utilization of only initial stiffness and moment capacity requires providing a mathematical representation of the moment-rotation

response, for the sake of the numerical analysis procedures.

Several mathematical models have been successfully used for that purpose, including but not limited to; multi-linear models, polynomial models, and power models such as three-parameter model (Kishi-Chen) [6], four-parameter model (Richard-Abbott) [33] and Ramberg-Osgood model [34]. Each has its advantages and limitations. Full details about these models are stated in Refs. [1, 2].

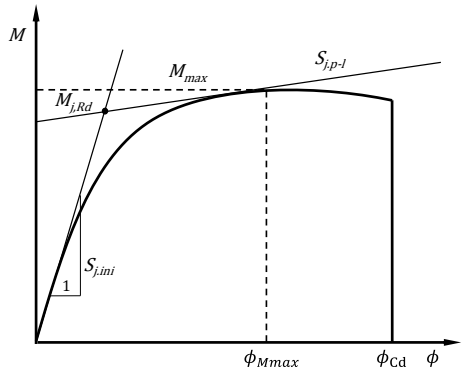

Figure 14: Typical moment-rotation response of steel connections.

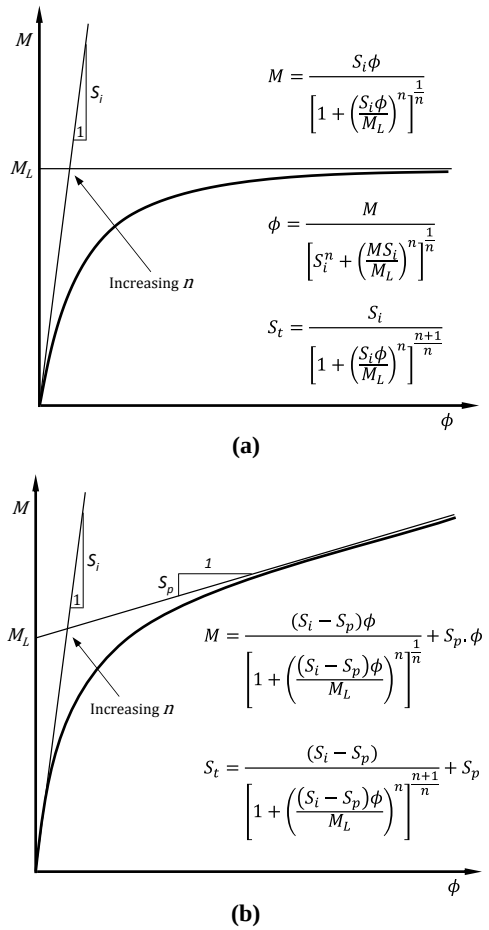

Figure 15: Connections power models; (a) three-parameter model, and (b) four-parameter model.

It is focused herein on the two power models because of their simplicity and suitability for numerical analysis: the three-parameter model, and the four-parameter model, as illustrated in Figure 15.

Both models are efficient and can be utilized in numerical analysis as they consider the gradual yielding of the connection. The latter enables considering the plastic portion of the curve which is represented by the post-yield rotational stiffness $S_{j.p-l}$ while the former does not require the value of the post-yield stiffness to represent the moment-rotation curve. However, the ratio of the post-yield stiffness to the initial stiffness $S_{j.p-l}/S_{j.ini}$ is too difficult to be predicted using the analytical approaches and needs to be reasonably assumed on the basis of experimental results from the knowledge of the connection's response at ambient temperature [32, 35].

Equations (5) and (6), as found in [6], give the moment-rotation function and the tangential stiffness according to the three-parameter model, respectively; while Equations (7) and (8) similarly represent the four-parameter model [33].

$$M = \frac{S_i\phi}{\left[1+\left(\frac{S_i\phi}{M_L}\right)^n\right]^{\frac{1}{n}}} \tag{5}$$

$$S_t = \frac{S_i}{\left[1+\left(\frac{S_i\phi}{M_L}\right)^n\right]^{\frac{n+1}{n}}} \tag{6}$$

$$M = \frac{(S_i-S_p)\phi}{\left[1+\left(\frac{(S_i-S_p)\phi}{M_L}\right)^n\right]^{\frac{1}{n}}} + S_p.\phi \tag{7}$$

$$S_t = \frac{(S_i-S_p)}{\left[1+\left(\frac{(S_i-S_p)\phi}{M_L}\right)^n\right]^{\frac{n+1}{n}}} + S_p \tag{8}$$

where,

M, ϕ are connection moment and the corresponding rotation, respectively.

S_t, S_i, S_p are the tangential, initial, and post-yield rotational stiffnesses, respectively.

M_L, n are reference (limiting) moment and curve sharpness (shape) parameter, respectively.

For the three-parameter model, the reference moment M_L is simply the moment capacity of the connection, while it can be calculated for the four-parameter model as follows:

$$M_L = M_{max} - S_p.\phi_{cd} \tag{9}$$

In the previous section, the proposed formulae showed good estimation of both initial stiffness and moment capacity. Yet, the other parameters (i.e., post-yield stiffness and curve sharpness parameter) need to be evaluated. This can be done by means of calibration with other model or experiment [35, 36].

Figure 16 compares the utilization of both three-parameter and four-parameter models with the experimental results of Ostrander – Test 1 [32] using the previously estimated initial stiffness and moment capacity. The three-parameter model compares well using $n = 1.5$, while the four-parameter model excellently fits the test results with $n = 1.5$ and $S_p = 0.01S_i$.

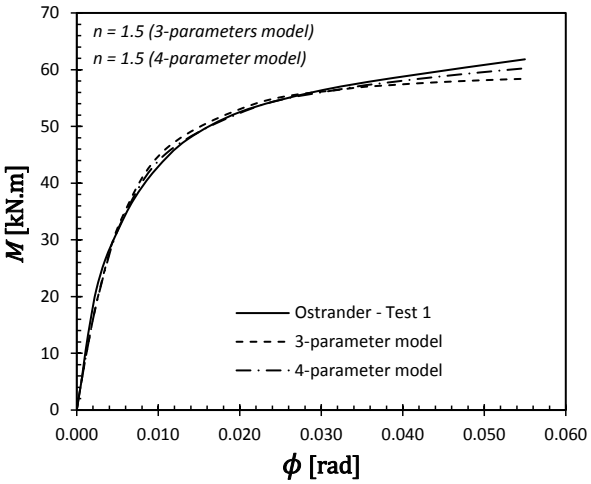

Figure 16: Mathematical representation of "Ostrander – Test 1" [32].

Similarly, the two models fits well with Graham – Test CS1-1 [28] in Figure 17 using $n = 0.8$ for the three-parameter model, and ($n = 0.7$ and $S_p = 0.01S_i$) for the four-parameter model.

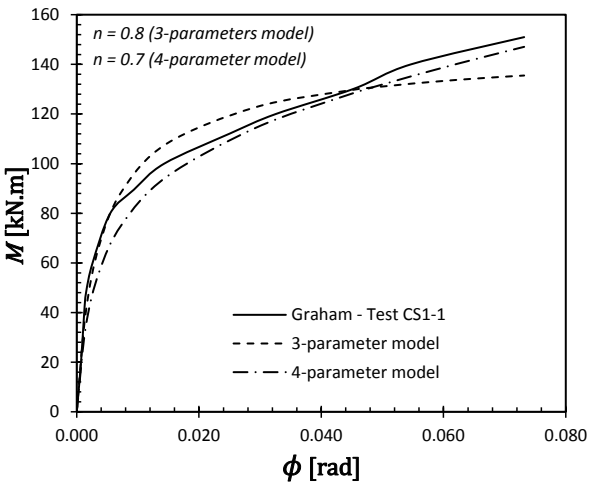

Figure 17: Mathematical representation of "Graham – Test CS1-1" [32].

Clearly, the four-parameter model is more flexible than the three-parameter model for curve fitting. However, in the absence of a reference curve to calibrate with, Hasan *et. al*. [36] recommended using the three-parameter model with shape parameter $n = 1$ as it is simpler and provides sufficient accuracy.

4. PROPOSED MOMENT-ROTATION CURVE AT ELEVATED TEMPERATURES

In the past few decades, several studies emphasized on the need to consider the behavior of steel connections at fire temperatures [25, 23, 24] as the reduced stiffness and strength of the connections undoubtedly affect the global response of the structure. Besides, the analysis of a bare steel structure exposed to fire necessitates considering numerous temperature distributions, according to the assumed fire scenarios [37]. Hence, it becomes very beneficial to extend the proposed formulae to account for the impact of temperature rise on connection characteristics.

4.1. Material Degradation at Elevated Temperatures

It is well known that temperature rise causes material deterioration in terms of stiffness and strength. Figure 18 shows the material reduction factors with temperature according to Eurocode [38], where $k_{y,\theta}$ and $k_{E,\theta}$ are the yield strength and Young's modulus reduction factors for carbon steel, respectively, and $k_{b,\theta}$ is the strength reduction factor for bolts.

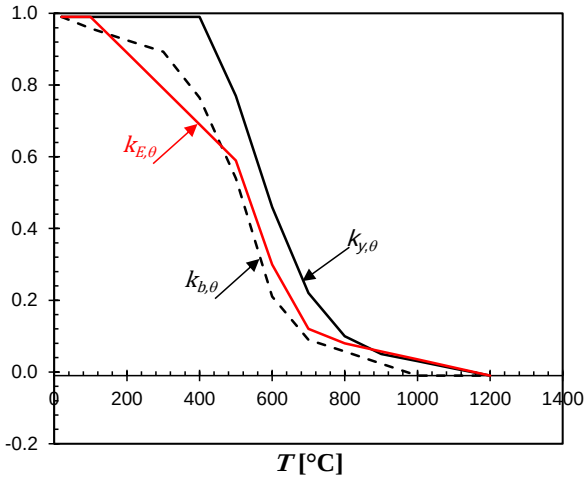

Figure 18: Strength reduction factors with temperature of carbon steel and bolt, EC3 [38].

In the present study, material degradation is represented by the factors; $R_E(T)$ and $R_f(T)$ which are the reduction factors for the Young's modulus and effective yield stress, respectively. These factors were recommended by other studies [37, 39] as they are merely an approximation of the Eurocode factors with slight modifications. Figure 19 shows the graphical

representation of these factors while Equations (10) and (11), respectively, provides the mathematical representation of the factors $R_E(T)$ and $R_f(T)$.

$$R_E(T) = \frac{20 - T}{1200} + 1.0 \qquad \text{for } 20°C < T \leq 500°C$$

$$R_E(T) = \frac{500 - T}{425.5} + 0.6 \qquad \text{for } 500°C < T \leq 700°C$$

$$R_E(T) = \frac{700 - T}{3846} + 0.13 \qquad \text{for } 700°C < T \leq 1200°C \tag{10}$$

$$R_f(T) = \frac{20 - T}{6229.5} + 1.0 \qquad \text{for } 20°C < T \leq 400°C$$

$$R_f(T) = \frac{400 - T}{419.58} + 0.939 \qquad \text{for } 400°C < T \leq 700°C$$

$$R_f(T) = \frac{700 - T}{877.2} + 0.224 \qquad \text{for } 700°C < T \leq 800°C$$

$$R_f(T) = \frac{800 - T}{3636.36} + 0.11 \qquad \text{for } 800°C < T \leq 1200°C \tag{11}$$

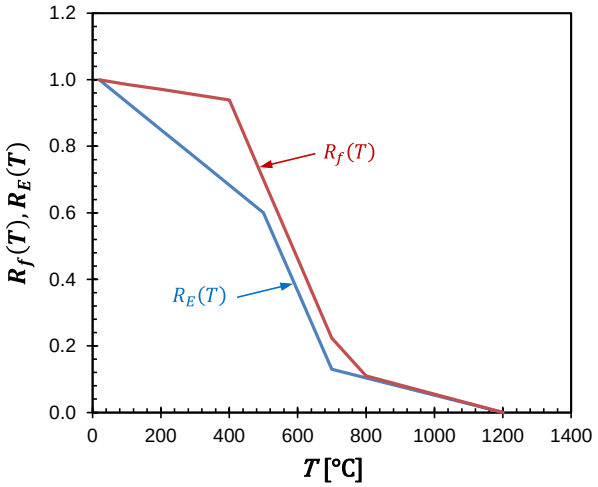

Figure 19: Material reduction factors $R_E(T)$ and $R_f(T)$ [39].

4.2. Connection Characteristics at Elevated Temperatures

For bare-steel connections, previous studies have shown that there is no appreciable difference in the temperature distribution across the connection [25, 24]. Accordingly, a uniform temperature field over the entire connection is assumed in the present study.

Taking into account that Equations (3) and (4) involve explicit material parameters f_y and f_{ub}, the connection characteristics at certain temperature can be estimated assuming that it is a new connection with lower steel grade (i.e., reduced Young's modulus and yield strength due to temperature rise). In other words, the moment capacity at an elevated temperature can be simply calculated by reducing the values of f_y and f_{ub} in Equations (3) and (4) using the Eurocode reduction factors as follows:

$$M_{j.Rd}(T) = a.[k_{y,\theta}.f_y]^b.h_b^c.t_{fc}^e.[k_{b,\theta}.f_{ub}]^f.d^g.t_p^h \tag{12}$$

$$S_{j.ini}(T) = k_{E,\theta}.[k.h_b^l.t_{fc}^m.d^u.t_p^o + q] \tag{13}$$

Alternatively, previous studies revealed that the initial stiffness of a connection is directly proportional to Young's modulus of steel at both ambient and elevated temperatures and the reduction in the estimated moment capacity of connections follows *directly* the reduction in yield strength with temperature increase [25, 23, 40]; hence, the moment capacity and initial stiffness of a connection at temperature T is to be calculated, using the recommended reduction factors, as:

$$M_{j.Rd}(T) = R_f(T).M_{j.Rd}(20) = R_f(T).[a.f_y^b.h_b^c.t_{fc}^e.f_{ub}^f.d^g.t_p^h] \tag{14}$$

$$S_{j.ini}(T) = R_E(T).S_{j.ini}(20) = R_E(T).[k.h_b^l.t_{fc}^m.d^u.t_p^o + q] \quad (15)$$

where $M_{j.Rd}(T)$ and $S_{j.ini}(T)$ are the estimated moment capacity and initial stiffness at temperature T, respectively.

In order to compare the estimated moment capacity using different strength reduction factors for connection parts and bolts according to Equation (12) with that obtained by Equation (14) assuming unified strength reduction factor, the moment capacities of two FEP and EEP connections with arbitrary configurations, previously referred at subsection 2.5 as Ostrand – Test 1 and de Lima – Test 2004, are calculated at temperatures range from 20 ℃ to 800 ℃. The results were normalized by relating the estimated moment capacity at temperature T, $M_{j,Rd}(T)$, to that associated with ambient temperature, $M_{j,Rd}(20)$. The comparison is illustrated graphically in Figure 20 where Equation (14) is represented implicitly by the reduction factor function of yield strength, $R_f(T)$ (continuous solid line), and the results obtained by Equation (12) are scattered. It can be noticed that Equation (14) overestimates the moment capacity beyond roughly 300 ℃ compared to the results calculated using Equation (12). However, a unified material reduction factor can be used conservatively for all connection parts, including high strength bolts, in predicting moment capacity at elevated temperatures [23, 25]; the recommended reduction factors can be used with some approximation to maintain simplicity of the model.

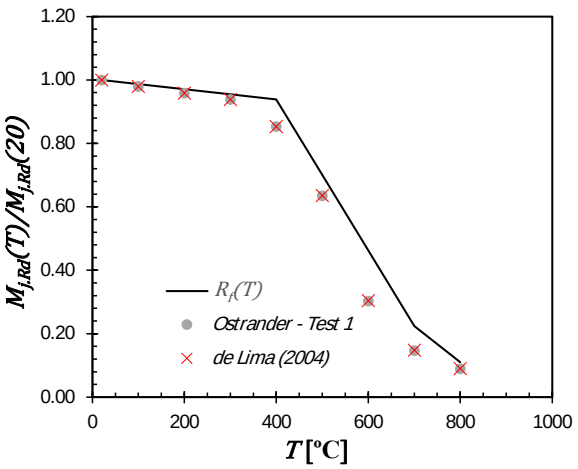

Figure 20: Comparison between the accuracy of Equations (12) and (14) on moment capacity prediction at elevated temperatures.

4.3. Application to Internal FEP Steel Connection

In order to validate the proposed formulae, the configuration and analysis results of flush end-plate steel joint previously tested by Al-Jabri *et al.* [24] is used. This cruciform joint configuration consists of two UB 254×102×22 beams connected to a UC 152×152×23 column by 8 mm thick flush end plates, as detailed in Figure 21.

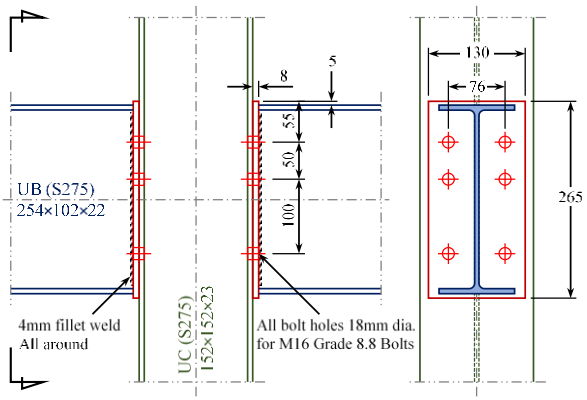

Figure 21: Details of cruciform FEP connection [24].

Four situations were tested under anisothermal conditions (i.e., increasing temperature under constant load level). The load levels were corresponding to different ratios of the calculated moment capacity at ambient temperature. Afterwards, the moment–rotation–temperature data collected from the tests were fitted using a modified Ramberg–Osgood expression [34] as follows:

$$\phi = \frac{M}{A} + 0.01\left(\frac{M}{B}\right)^n \quad (16)$$

where,

A, B *and* n are temperature dependent parameters.

The proposed formulae are used for estimating the initial rotational stiffness and moment capacity of that connection configuration at different temperature stations. Then, using those characteristics, the moment-rotation curves are mathematically generated using three-parameter and four-parameter models at each temperature. Figures 22 and 23 compare the predicted response of the connection using the proposed technique against Al-Jabri's equations.

It is realized that the proposed technique provides good estimation and representation of the connection response over the entire temperature range. In addition to its simplicity, the three-parameter model tends to be more conservative than the four-parameter model. Moreover, the required calibration was limited to defining the ratio of the post-yield stiffness to the initial stiffness $S_{j.p-l}/S_{j.ini}$ and the shape parameter n. Table 7 ists those parameters over the covered temperature range.

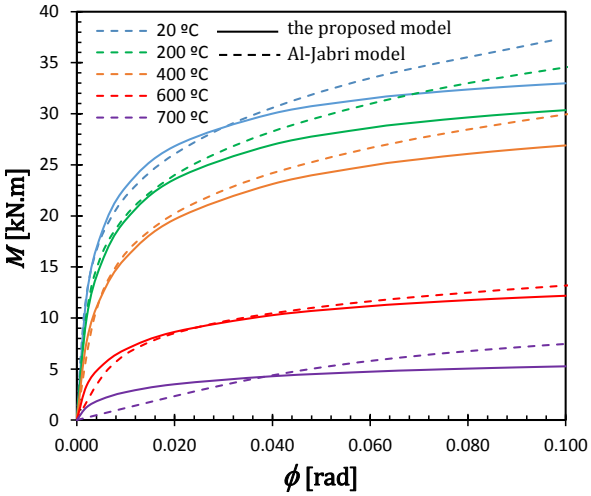

Figure 22: Predicted moment-rotation-temperature curves using the proposed formulae (solid lines) vs. Al-Jabri equations [24] (dashed lines), three-parameter model.

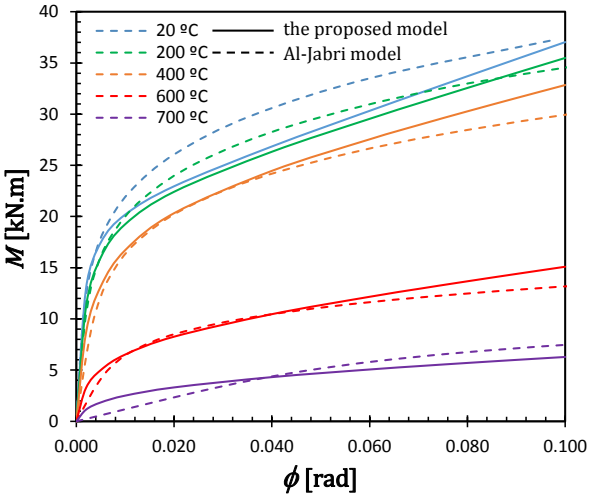

Figure 23: Predicted moment-rotation-temperature curves using the proposed formulae (solid lines) vs. Al-Jabri equations [24] (dashed lines), four-parameter model.

Table 7. Required parameters for calibration of the connection response.

Model	Parameter	T, ℃				
		20	200	400	600	700
Three-parameter model	n	0.66	0.60	0.54	0.48	0.45
Four-parameter model	n	1.00	0.86	0.70	0.54	0.46
Four-parameter model	$S_{j.p-l}/S_{j.ini}$			0.01		

Implementation of this technique in practical nonlinear analysis requires an incremental procedure with relatively small temperature jumps so that the mechanical properties of the connection remain constant during each temperature interval. For the sake of computer modeling, the proposed Equations (17) and (18) provide simple representation of the shape parameter n as a function of temperature.

$$n = 0.661 - 0.0003\,T \text{ (three-parameter model)} \quad (17)$$

$$n = 1.016 - 0.0008\,T \text{ (four-parameter model)} \quad (18)$$

Unfortunately, in addition to the required calibration at ambient temperature, each connection configuration needs further calibration at elevated temperatures [24]. This could increase the complexity of the prediction of connection response at fire scenarios. To overcome this downside, many studies recommended more investigation on connection behavior at elevated temperatures via experimental tests and extensive numerical simulations.

5. ILLUSTRATIVE EXAMPLE

In order to put all together, the proposed procedure has been included into a Structural-Thermal Analysis Program, STAP, which is based on direct-stiffness analysis software presented by Nassef [41]. This software utilizes the effective tangent modulus concept and has been detailed and validated against experimental tests as well as against more complex finite element models showing good accuracy and low analysis times [37, 39, 42]. To perform the present study, special modules were added to the program to compute the end-plate connection parameters based on the proposed equations and the connection moment-rotation curve was then constructed. The member end connections were presented in the analysis in the form of nonlinear springs with tangent stiffnesses deduced from the computed moment rotation curves. Finally, the stiffness matrix for the conventional beam-column element shown in Figure 24 was modified following Monforton's formulation [43] to account for the end-springs simulating the semi-rigid connection behavior.

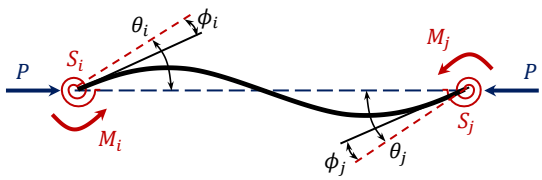

Figure 24: Beam-column element with end springs.

The program was thereafter able to carry out nonlinear analysis in which the nonlinearity came from the connection semi-rigidity and connection and member stiffnesses degradation due to elevated temperature.

The rugby goal-post frame shown in Figure 25 was numerically analyzed by Dong [44] using Vulcan software. The frame consists of two UC203×203×71 columns and UB254×102×22 beam with depicted dimensions.

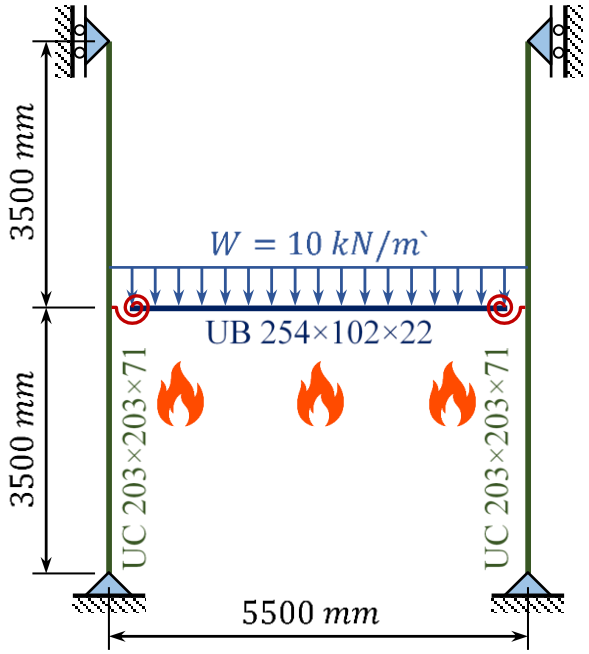

Figure 25: 2D "rugby goal-post" frame, Dong [44].

The beam is connected to columns by two semi-rigid flush end-plate connections with end plate of 12 mm thickness and two 10.9 M12 bolts. All frame elements and connections are of S275 grade. Only the beam is uniformly heated including the end connections and the mid-span deflection was monitored with temperature growth. The frame was re-analyzed using the proposed models to track the designated deflection and determine the failure temperature. The analysis proceeded based on 100 °C temperature stations until the frame approaches its failure temperature; the temperature is then increased at finer increments until the frame fails. Equations (14) and (15) are used to calculate the connection characteristics at each temperature stations; the three-parameter model is implemented to generate the moment-rotation curve using Equations (5) and (6) with shape parameter $n = 1$ for the entire temperature range. The frame has collapsed due to beam failure at temperature of 660 ºC. The tracked deflection is depicted in Figure 26 and compared to Dong's results. Good agreement was achieved using the proposed procedure with much lower computational effort.

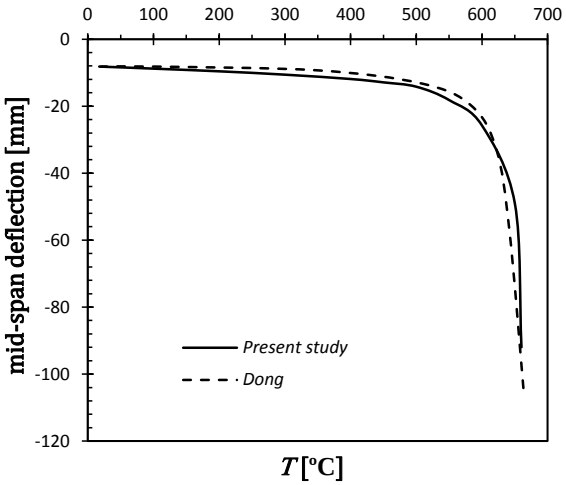

Figure 26: Comparison of mid-span deflection of Dong's frame with the proposed procedure.

6. SUMMARY AND CONCLUSIONS

This study proposes a full numerical procedure of predicting the moment-rotation curve for moment-resistant connections, end-plate type, at both ambient and elevated temperatures. The simplicity of the proposed procedure provides researchers and practitioners with comprehensive information when addressing structural problems involving semi-rigid behavior of end-plate connections at fire conditions. The proposed model is essentially based on regression analysis of data generated by the application of the Eurocode component method (CM) on wide and practical range of connection configurations, showing very good accuracy as a direct alternate to the stepwise application of CM. Proper selection of the key predictive parameters, especially the explicit material parameters, gives the proposed model an advantage over the other models which either restricted with dimensional and geometrical constraints or limited to specific steel grade. Moreover, the proposed formulae are applicable in both ambient and elevated temperature conditions. The full moment-rotation curve of a connection can be produced by incorporating the predicted characteristics (initial rotational stiffness and moment capacity) into a suitable power model with proper calibration. Equations (17) and (18) provide an example for calibration of moment-rotation curve for tested FEP connection at elevated temperatures. However, due to the lack of test data of connections at elevated temperature, the shape parameter n can be considered equal to unity over the entire temperature range as shown in the illustrative example (Figure 26).

The proposed formulae have been validated against previous experimental test data showing reasonable estimations at both ambient and elevated temperatures. In addition, the proposed technique has been tested in a full numerical analysis via an illustrative example and showed good results with relatively low computational

time. Finally, the proposed technique combines the simplicity of data input, fast building of the structural model, and good accuracy of the results when compared with the complex three-dimensional finite element models.

In addition to model validation, the following conclusions can be drawn from the study presented herein.

- The proposed predictive formulae provide initial reasonable estimation of connection characteristics and the proposed moment-rotation models can be incorporated in any numerical stiffness-based nonlinear frame analysis at ambient or elevated temperatures as an efficient alternate to laborious FE analysis, especially in the preliminary analysis phase; it provides acceptable accuracy regarding its low computational time and simplicity of construction of the structural model with minimal amount of input data.
- Although the four-parameter model which requires additional calibration for the post-yield rotational stiffness gives more realistic tracking of the moment-rotation relationship, but the three-parameter model gives good results without the need of the fourth parameter. Moreover, using the same post-yield stiffness to the initial stiffness ratio $S_{j.p-l}/S_{j.ini}$ at both ambient and elevated temperatures fits well in the application of the four-parameter model.

Further calibration of the moment-rotation curves is essentially required at elevated temperature situations. Accordingly, more test data of heated connections must be provided for more prediction reliability.

7. REFERENCES

[1] S. L. Chan and P. T. Chui, Non-linear static and cyclic analysis of steel frames with semi-rigid connections, Elsevier, 2000.

[2] C. Díaz, P. Martí, M. Victoria and O. Querin, "Review on the modelling of joint behaviour in steel frames," *Journal of constructional steel research,* vol. 67, pp. 741-58, 2011.

[3] D. M, R. Tartaglia, S. Costanzo and R. Landolfo, "Seismic design of extended stiffened end-plate joints in the framework of Eurocodes," *Journal of Constructional Steel Research,* vol. 128, pp. 512-527, 2017.

[4] T. Yin, Z. Wang, J. Pan, K. Zheng, D. Liu and S. Lu, "A Design Method for Semi-Rigid Steel Frame via Pre-Established Performance-Based Connection Database," *Buildings,* no. 12, p. 1634, 2020.

[5] A. G. Coelho and F. S. Bijlaard, "Behaviour of high strength steel moment joints," *Heron,* vol. 55, no. 1, pp. 1-32, 2010.

[6] N. Kishi and W. Chen, "Moment-rotation relations of semirigid connections with angles," *Journal of Structural Engineering,* vol. 116, pp. 1813-1834, 1990.

[7] N. Kishi and W. Chen, "Data base of steel beam-to-column connections," *Structural Engineering Area, School of Civil Engineering, Purdue University,* 1986.

[8] K. Abdalla and W. Chen, "Expanded database of semi-rigid steel connections," *Computers & Structures,* vol. 56, no. 4, pp. 553-564, 1995.

[9] K. Weynand, M. Huter, P. Kirby, L. Simoes da Silva and P. Cruz, "SERICON–Databank on Joints in Building Frames," *InProceedings of the 1st COST C1 Workshop 1992 Oct 28,* pp. 28-30.

[10] P. Cruz, L. da Silva, D. Rodrigues and R. Simões, "Database for the semi-rigid behaviour of beam-to-column connections in seismic regions," *Journal of Constructional Steel Research,* vol. 46, no. 1, pp. 233-234, 1998.

[11] M. Frye and G. Morris, "Analysis of flexibly connected steel frames," *Canadian Journal of Civil Engineering,* vol. 2, no. 3, pp. 280-291, 1975.

[12] Z. Ding and A. Elkady, "Semirigid Bolted Endplate Moment Connections: Review and Experimental-Based Assessment of Available Predictive Models," *Journal of Structural Engineering,* vol. 149, no. 9, p. 04023117, 2023.

[13] N. Krishnamurthy, "Fresh look at bolted end-plate behaviour and design," *Engineering Journal,* vol. 15, no. 2, pp. 39-49, 1978.

[14] N. Krishnamurthy, H. Huang, P. Jeffrey and L. Avery, "Analytical M-θ curves for end-plate connections," *Journal of the Structural Division,* vol. 105, no. 1, pp. 133-145, 1979.

[15] A. Kozlowski, R. Kowalczyk and M. Gizejowski, "Estimation of the initial stiffness and moment resistance of steel and composite joints," *In CTBUH 8th World Congress, Dubai Mar 3-5,* 2008.

[16] G. Terracciano, G. Della Corte, G. Di Lorenzo and R. Landolfo, "Design Tools for Bolted End-Plate Beam-to-Column Joints," *Journal of Engineering,* vol. 1, p. 9689453, 2018.

[17] M. Eladly and B. Schafer, "Numerical and analytical study of stainless steel beam-to-column extended end-plate connections," *Engineering Structures,* vol. 240, p. 112392, 2021.

[18] Z. Kong, S. Hong, Q. Vu, X. Cao, S. Kim and B. Yu, "New equations for predicting initial stiffness and ultimate moment of flush end-plate connections," *Journal of Constructional Steel Research,* vol. 175, p. 106336, 2020.

[19] A. Kueh, "Artificial neural network and regressed beam-column connection explicit mathematical moment-rotation expressions," *Journal of Building Engineering,* vol. 43, no. 1, p. 103195, 2021.

[20] G. Georgiou and A. Elkady, "ANN-Based Model for Predicting the Nonlinear Response of Flush Endplate Connections," *Journal of Structural Engineering,* vol. 150, no. 5, p. 04024034, 2024.

[21] M. Shaheen, A. Foster, L. Cunningham and S. Afshan, "Behaviour of stainless and high strength steel bolt assemblies at elevated temperatures—A review," *Fire Safety Journal,* vol. 113, p. 102975, 2020.

[22] Z. Ding and A. Elkady, "Accuracy assessment of predictive models for semirigid extended end-plate connections," *ce/papers 6, no. 3-4,* pp. 1263-1268.

[23] J. A. El-Rimawi, I. W. Burgess and R. J. Plank, "The influence of connection stiffness on the behaviour of steel beams in fire," *Journal of constructional steel research,* vol. 43, no. 1-3, pp. 1-15, 1997.

[24] K. S. Al-Jabri, I. W. Burgess, T. Lennon and R. J. Plank, "Moment–rotation–temperature curves for semi-rigid joints," *Journal of Constructional Steel Research,* vol. 61, p. 281–303, 2005.

[25] L. S. Da Silva, A. Santiago and P. V. Real, "A component model for the behaviour of steel joints at elevated temperatures," *Journal of Constructional Steel Research,* vol. 57, no. 11, pp. 1169-1195, 2001.

[26] Moment-Resisting Joints to Eurocode 3, The Steel Construction Institute, The British Constructional Steelwork Association, 2013.

[27] Eurocode 3: Design of steel structures-Part 1-8: Design of joints. BS EN 1993-1-8, 2005.

[28] L. R. de Lima, L. S. da Silva, P. D. Vellasco and S. A. De Andrade, "Experimental evaluation of extended end-plate beam-to-column joints subjected to bending and axial force," *Engineering Structures,* vol. 26, p. 1333–1347, 2004.

[29] A. M. Coelho, F. S. Bijlaard and L. S. da Silva, "Experimental assessment of the ductility of extended end plate connections," *Engineering Structures,* vol. 26, no. 9, p. 1185–1206, 2004.

[30] M. Steenhuis, N. Gresnigt and K. Weynand, "Pre-design of semi-rigid joints in steel frames," *In Proceedings of the Second State of the Art Workshop on Semi-Rigid Behaviour of Civil Engineering Structural Connections,* pp. 131-140, 1994.

[31] "IBM Corp. Released 2019. IBM SPSS Statistics for Windows, Version 26.0. Armonk, NY: IBM Corp".

[32] Z. Benterkia, "End-plate connections and analysis of semi-rigid steel frames," *Doctoral dissertation, University of Warwick,* 1991.

[33] R. Richard and B. Abbott, "Versatile elastic-plastic stress-strain formula," *Journal of the Engineering Mechanics Division,* vol. 101, pp. 511-515, 1975.

[34] W. Ramberg and W. Osgood, "Description of stress–strain curves by 3 parameters," *Technical Report 902, National Advisory Committee for Aeronautics,* 1943.

[35] M. Chmielowiec, Moment rotation curves for partially restrained steel connections, The University of Arizona, 1987.

[36] R. Hasan, N. Kishi and W. Chen, "A new nonlinear connection classification system," *Journal of Constructional Steel Research,* vol. 47, pp. 119-140, 1998.

[37] A. ElSabbagh, W. Nassef, M. El-Ghandour and T. Sharaf, "Inelastic buckling analysis of steel columns at different fire scenarios," *Engineering Structures,* vol. 291, p. 116464, 2023.

[38] Eurocode 3: Design of steel structures-Part 1-2: General rules–structural fire design. BS EN 1993-1-2, 2005.

[39] M. A. Mohamadain, I. A. El-Arabi and W. M. Nassef, "Simplified nonlinear analysis of steel frames at elevated temperatures," *The bulletin of the Faculty of Engineering Ain Shams University, Cairo, Egypt,* pp. 215-8, 2010.

[40] F. Block, "Development of a component-based finite element for steel beam-to-column connections at elevated temperatures," *Doctoral dissertation, University of Sheffield,* 2006.

[41] W. M. Nassef, "Behavior of structural systems at elevated temperatures," *M.Sc. Thesis, Port Said University,* 2010.

[42] M. A. Mohamadain, I. A. El-Arabi and W. M. Nassef, "Inelastic stability of steel trapezoidal frames at elevated temperatures," *Ain Shams Engineering Journal,* vol. 1, no. 1, pp. 21-30, 2010.

[43] G. Monforton, "Matrix analysis of frames with semi-rigid connections," *B.A.Sc., Assumption University of Windsor,* 1961.

[44] G. Dong, "Development of a General-Purpose Component-based Connection Element for Structural Fire Analysis," *(Doctoral dissertation, University of Sheffield),* 2016.